AIAA JOURNAL
Vol. 34, No. 2, February 1996

Finite Element Model Tuning Using Automated Structural Optimization System Software

Richard G. Cobb,* Robert A. Canfield,† and Brad S. Liebst‡
U.S. Air Force Institute of Technology, Wright–Patterson Air Force Base, Ohio 45433-7765

A method of adjusting analytical finite element models to measured data is presented. The algorithm uses a mathematical optimization strategy to minimize deviations between measured and analytical modal frequencies and partial mode shapes. A mode tracking algorithm is used to identify and account for mode switching during the optimization process. The algorithm was successfully implemented using the Automated Structural Optimization System Software. Experimental results are presented for tuning a lightly damped 6-m flexible frame structure. The results demonstrate excellent agreement between the tuned model and measured data and illustrate the importance of off-nominal validation before accepting a model for simulation purposes.

Introduction

ACCURATE prediction and simulation of the dynamic behavior of large flexible space structures require analytical models that agree with measured data. Unfortunately, uncertainty in a finite element model (FEM) implies less than perfect correlation between analytical and measured data. When the disagreement is deemed unacceptable, it is necessary for the design engineer to make adjustments to the FEM. For large problems the number of potential parameters to adjust, such as elemental areas, elastic moduli, inertia moments, etc., quickly becomes overwhelming. Thus a systematic method is required to ensure the adjustments produce the desired results. To this end, a method is introduced that poses a numerical optimization problem, namely, given a set of measured eigenvalues and partial eigenvectors, determine the values of selected physical parameters of the model that minimize the weighted deviations from the analytical eigenvalues and eigenvectors.

Numerous techniques and goals of model tuning, also referred to as model refinement or model identification, have appeared in the literature. The common attribute of these techniques is that they attempt to minimize the required modification to the analytical mass and stiffness matrices, assuming the FEM is a reasonable approximation to the physical structure. Sensitivity based approaches have been presented in the literature that adjust the matrices by establishing an objective function based on the difference between the experimental and analytical model data.[1–5] An advantage of those methods is that the updated models are consistent with the FEM formulation, and thus the connectivity is preserved. An alternative method employing an optimal matrix update has been developed by Berman and Nogy[6] and Baruch.[7] In this method, a perturbation mass, damping, or stiffness matrix is determined that, when added to the analytical matrices, produces the measured result. The advantage of this method is a tuned analytic model that exactly reproduces the experimental data. Its shortcoming is that it does not guarantee the closeness to unmeasured modes not used in the tuning process. This is a result of potentially unrealistic changes in the stiffness matrix, such as the introduction of load paths that physically do not exist. To overcome some of the shortcomings of Baruch's method of stiffness matrix adjustments, Kabe[8] and Kammer[9] introduced objective functions that ensure stiffness terms are corrected in a manner such that the connectivity of the analytical model is preserved. Similar work has been investigated by Smith and Beattie.[10] Another approach that has been applied to model tuning is the residual force approach. This technique, developed by Chen and Garba, is based on computation of a residual vector that represents the mismatch between the analytical model and the modal data.[11] By examining the mismatch, the engineer should be able to locate the errors in the model and then modify the model.

A critical aspect to any model tuning algorithm is its practical implementation. Key advantages to the method presented herein include its ability to handle a small subset of the total eigenstructure of the system without using an eigenvector expansion method and the ability to track mode switches during the tuning process. This optimization strategy was implemented using the Automated Structural Optimization System (ASTROS) software package developed by Wright Laboratory.[12] The present research work is an extension to the work begun by Gibson on the software modules ASTROS-ID, an enhancement to ASTROS to incorporate system identification.[13] The overall intent of this software enhancement is to enable the user to input a set of desired modal frequencies and partial modal vectors and then iterate on a set of structural parameters to minimize deviations between analytical and experimental measurements. This paper documents an enhanced methodology to perform the optimization and presents experimental results. A FEM of a 6-m frame assembly composed of 100 elements was successfully tuned using this procedure.

Theory

Model tuning is performed by minimizing an objective function based on a weighted sum of deviations from measured eigenvalues and partial eigenvectors. Assuming real eigenvalues and eigenvectors, the objective function is given as

$$J = \sum_{i=1}^{p} a_i \left(\frac{\lambda_i}{\bar{\lambda}_i} - 1 \right)^2 + \sum_{i=1}^{q} \sum_{j=1}^{r} b_{ij} (\phi_{ij} - \bar{\phi}_{ij})^2 \qquad (1)$$

where the analytical eigenvalue for the ith mode is denoted as λ_i and ϕ_{ij} denotes the jth element of the ith eigenvector from the modal matrix Φ. The overbar indicates a measured quantity. The positive coefficients a_i and b_{ij} allow for individual weightings in the objective function. The summation upper limits p, q, and r represent the number of eigenvalues, eigenvectors, and elements of the eigenvectors, respectively, chosen to be tuned. The minimization of the objective function J is carried out in an inner and outer loop fashion. The outer loop consists of performing the eigenanalysis, normalizing and matching analytical and measured modes, calculating design parameter sensitivities, updating design variables, and detecting solution convergence. The inner loop solves an approximate optimization problem after each outer loop eigenanalysis using the new design variable sensitivity information. The inner loop is an approximate solution because the sensitivity information is used

Received June 16, 1995; revision received Sept. 9, 1995; accepted for publication Sept. 12, 1995.

*Graduate Student, Department of Aeronautics and Astronautics, Bldg. 640, 2950 P Street. Student Member AIAA.
†Assistant Professor, Department of Aeronautics and Astronautics, Bldg. 640, 2950 P Street. Senior Member AIAA.
‡Associate Professor, Department of Aeronautics and Astronautics, Bldg. 640, 2950 P Street. Senior Member AIAA.

to project new values of the analytical eigenvalues and eigenvectors for given changes in the design variables without recomputing the eigenanalysis. Once the approximate problem is solved by a general constrained optimization method, control is passed to the outer loop where the variables are updated and a new eigenanalysis is performed. The details of computing the sensitivity information as well as the mode normalization and tracking will be discussed next. The problem considered herein assumes real eigenanalysis and is not developed for the case where damping is included in the finite element formulation.

Eigenvalue Sensitivity

A second-order Taylor series expansion is used to project new eigenvalue values to given design variable changes contained in the vector $\Delta\nu$. The expansion is given as

$$\lambda_i \cong \lambda_{0i} + \nabla\lambda_i^T \Delta\nu + \tfrac{1}{2}\Delta\nu^T\left(\nabla^2\lambda_i\right)\Delta\nu \tag{2}$$

where λ_{0i} denotes the initial eigenvalue resulting from the eigenanalysis. The jth element of the eigenvalue gradient vector $\nabla\lambda_i$ is given as[14]

$$\lambda_{i,j} = \frac{\Phi_i^T[K_{,j} - \lambda_i M_{,j}]\Phi_i}{\Phi_i^T M \Phi_i} \tag{3}$$

where a comma denotes differentiation with respect to a design variable. The elements of the Hessian matrix $\nabla^2\lambda_i$ are given as

$$\lambda_{i,jk} = \frac{\Phi_i^T[F_{i,j}\Phi_{i,k} + F_{i,k}\Phi_{i,j}] - \left[\lambda_{i,j}\Phi_i^T M_{,k}\Phi_i + \lambda_{i,k}\Phi_i^T M_{,j}\Phi_i\right]}{\Phi_i^T M \Phi_i} \tag{4}$$

with $F_{i,j}$ defined as

$$F_{i,j} \equiv K_{,j} - \lambda_i M_{,j} - \lambda_{i,j} M \tag{5}$$

The notation $(\bullet)_{i,j}$ represents differentiation with respect to the jth design variable of some quantity$(\bullet)$, associated with the ith mode. The decision to include a second-order approximation, rather than only a first order, was due to the fact that the terms appearing in the second-order eigenvalue gradient are already computed when calculating the first-order eigenvector gradients. Equations (3) and (4) include the scalar normalization term $\Phi_i^T M \Phi_i$. Thus the eigenvector normalization will scale the eigenvalue gradients. Proper choice of eigenvector normalization is addressed in the next section. Design sensitivities of the mass and stiffness matrices M and K are known explicitly from the finite element formulation and can thus be computed using either analytical derivatives or finite difference methods. Eigenvalue sensitivity for each mode included in the objective function is computed according to Eqs. (3) and (4). The eigenvector derivatives in Eq. (4) can be computed by a modal expansion[15] or more efficiently by Nelson's method[16] when only a subset of eigenvectors are involved, as explained next.

Eigenvector Sensitivity and Normalization

A first-order Taylor series expansion is used to project the new value of the eigenvector based on the eigensolution value Φ_{0i} and the eigenvector gradient $\nabla\Phi_i$. The expansion is computed for each degree of freedom (DOF) in the measured eigenvector set. The expansion of the kth term of the eigenvector for the ith mode is given as

$$\phi_{ik} \cong \phi_{0ik} + \nabla\phi_{ik}^T \Delta\nu \tag{6}$$

The eigenvector gradient is found by first differentiating the eigenvalue equation for each mode with respect to each design variable:

$$[K - \lambda_i M]\Phi_{i,j} = [\lambda_{i,j} M + \lambda_i M_{,j} - K_{,j}]\Phi_i \tag{7}$$

Since the left-hand side is necessarily singular by definition, the solution to $\Phi_{i,j}$ is found by employing Nelson's method. The problem is solved by separating $\Phi_{i,j}$ into the sum of a particular and homogeneous solution given as

$$\Phi_{i,j} = c_{ij}\Phi_i + V_{ij} \tag{8}$$

Assuming there are no repeated roots, and $[K - \lambda_i M]$ is an $(N \times N)$ matrix, then its rank is $N - 1$. Thus the homogeneous solution is found by eliminating a row and column and then performing the inverse:

$$V_{ij} = [\tilde{K} - \lambda_i \tilde{M}]^{-1}[\lambda_{i,j}\tilde{M} + \lambda_i \tilde{M}_{,j} - \tilde{K}_{,j}]\tilde{\Phi}_i \tag{9}$$

The $(\tilde{\bullet})$ notation denotes matrices reduced by one row and column. Nelson's method removes the row and column corresponding to the maximum entry in Φ_i. Note that the matrix inverse in Eq. (9) need not be explicitly calculated; rather the reduced matrices can be used in Eq. (7) and solved through matrix decomposition and back substitution. To solve for the unknown scalar constant c_{ik} in Eq. (8), a normalization constraint must be applied. The objective of the optimization is to minimize differences between measured and analytical modes, which clearly can only be computed when the eigenvectors are normalized in the same manner. To achieve this objective, a point normalization scheme is used in which eigenvectors are normalized such that the DOF with maximum amplitude in the measurement set is set to unity. Presumably, this would also correspond to a DOF in which there was high measurement confidence (i.e., high signal/noise). This is important because the analytic gradient of this DOF will be identically zero. It is not practical nor useful for optimization to normalize eigenvectors based on the analytical model, such as by mass normalization, since the analytical matrices are the unknowns in the optimization routine. However, mass normalized analytical eigenvectors are useful in detecting mode switches and are discussed in the next section. After each eigenanalysis in the outer loop, the eigenvectors used in the objective function must be normalized per the measurement data. Having chosen the degree-of-freedom normalization point for each mode, the normalization constraint for each mode can be expressed as

$$\Phi_i^T S_i \Phi_i = 1 \tag{10}$$

where the matrix S_i contains only one nonzero entry, a one in the row and column corresponding to the normalization point for the ith mode. Differentiating the constraint Eq. (10) with respect to each design variable and substituting the result from Eq. (8) yields

$$\Phi_i^T S_i[c_{ij}\Phi_i + V_{ij}] = 0 \tag{11}$$

Because of the special form of the matrix S_i Eq. (11) simplifies to

$$c_{ij} = -(V_{ij})_{\text{norm.pt.}} \tag{12}$$

which is the negative of the element in vector V_{ij} corresponding to the normalization point for the ith mode. The point normalized eigenvectors must be used in calculating the term $\Phi_i^T M \Phi_i$ in Eqs. (3) and (4) to ensure proper scaling of the eigenvalue and eigenvector sensitivities. The eigenvector sensitivity is computed for each mode included in the objective function. For measured modes where only frequency information (not shape) is available, a first-order Taylor series expansion is used in lieu of Eq. (2).

Mode Switch Detection

For convenience, the engineer typically will assign a numbering scheme to the set of measured modes from an experimental analysis. It is imperative that the same numbering scheme be employed when comparing measured modes to analytical modes. Before the start of the optimization, this numbering scheme is most easily facilitated through the use of computer-aided software capable of displaying mode shapes. At this point, the designer can pair up measured and analytical modes. Once the optimization starts, however, it is necessary for the software to track the analytical mode sequencing. As the design variables change, it is highly likely that mode switching will occur. Without mode tracking, an optimization scheme would become hopelessly lost trying to match bending modes to torsion modes, for example, and vice versa. Mode tracking can be performed using cross-orthogonality checking.[13] If the eigenvectors are mass normalized, mode tracking can be accomplished by computing the modal correlation coefficient matrix between successive eigenanalysis solutions. The cross-orthogonality matrix is given as

$$C = \Phi^{(n-1)T} M^{(n)} \Phi^{(n)} \tag{13}$$

The modal matrix Φ includes only the eigenvectors computed in the eigenanalysis. The superscript n denotes the iteration number.

Assuming mass orthonormalization, near unity values in C indicate high correlation between modes. Mode tracking is accomplished by searching over C successively for the largest absolute value. If the entry is in a diagonal location, this mode has not changed between iterations. An absolute maximum in a nondiagonal entry indicates the mode number switch between two iterations by its row and column position. After each mode is paired, the corresponding row and column are eliminated from C, and the search for the next pair is accomplished on the reduced matrix until all modal pairs are found. As discussed previously, mode switch detection is done in the outer optimization loop, just before point normalization and eigensensitivity calculations.

Implementation and Design Variables

This model tuning technique was implemented using the structural design software ASTROS. This software uses an executive control sequence Matrix Analysis Problem Oriented Language (MAPOL) to develop the solution sequence. MAPOL allows the user to incorporate custom software modules into the solution sequence while maintaining full access to the ASTROS solution modules. For the problem at hand, software modules written in Fortran 77 were developed (or modified from Gibson's original work) for eigenvector normalization, mode switch testing, eigenvalue and eigenvector sensitivities, objective function evaluation, and processing data to and from the optimization module. A small section of MAPOL code is then inserted into the standard ASTROS solution sequence to control the calling of these new modules. Tuning information (desired frequencies, mode shapes, and the corresponding weighting values) are appended to the standard bulk data input. Additional information on the use of ASTROS as a multidisciplinary design tool can be found in the literature.[17,18]

Before the optimization can be performed, the designer must choose a set of design variables. In ASTROS, the design variable for a beam element is the beam's cross-sectional area, because weight minimization is typically the overall objective. In model tuning, however, other properties such as the elastic moduli, mass, or both may be the desired design variables. To accommodate the ability to tune more than one property of an element, superposition can be used. To illustrate this method, consider tuning the mass and elastic modulus of a beam between two nodes. Using two beam elements, one with the elastic modulus set to zero and a second with the density property set to zero, will have the combined effect of a single beam element. However, now both properties can be set as design variables. Note that adjusting the cross-sectional area of a beam with a zero elastic modulus is equivalent to adjusting the density property of that beam. A similar relation is true for the beam element with zero mass density. In a similar fashion, the torsional properties of the beam can be varied independently. Using this technique allows the user a wide choice of design variables.

Selection of which design variables to vary is dependent on the designer's objective and is problem dependent. If in the development of the finite element model some of the more complicated geometries where simplified using equivalent but uncertain parameters, then these parameters are the natural choice for the design variables. If, however, the objective is damage location identification, then design variables must be chosen that relate directly to damaged elements. An additional consideration in design variable selection is how changes in the design variables affect the mass and inertia properties of the structure. To accommodate tuning the model to a desired mass, an additional term was appended to the objective function in Eq. (1), representing the error between the tuned and target mass values. Additional terms can also be appended to achieve a desired center of gravity location and moments of inertia, as required.

Experimental Results

The 6-m flexible truss experiment (FTE) was assembled at the Air Force Institute of Technology from excess hardware received from the Structural Dynamics Branch of Wright Laboratory after termination of the 12-m truss active control experiment.[19] The hardware consists of the truss assembly, actuators and their power drivers, accelerometer sensors, and real-time digital control and signal processing equipment. As presented in the documentation on the 12-m truss, there was considerable difficulty in obtaining a model of the 12-m truss that correlated well with measured data. Although only half the structure is currently used because of physical space limitations, the difficulty in modeling the structure makes it ideally suited to use in validating a model tuning algorithm. It should also be noted that the experiment's name is somewhat of a misnomer. Although the word truss is used, the structure is actually a frame structure with rigid connections between members. The term truss typically is used for structures with pinned connections.

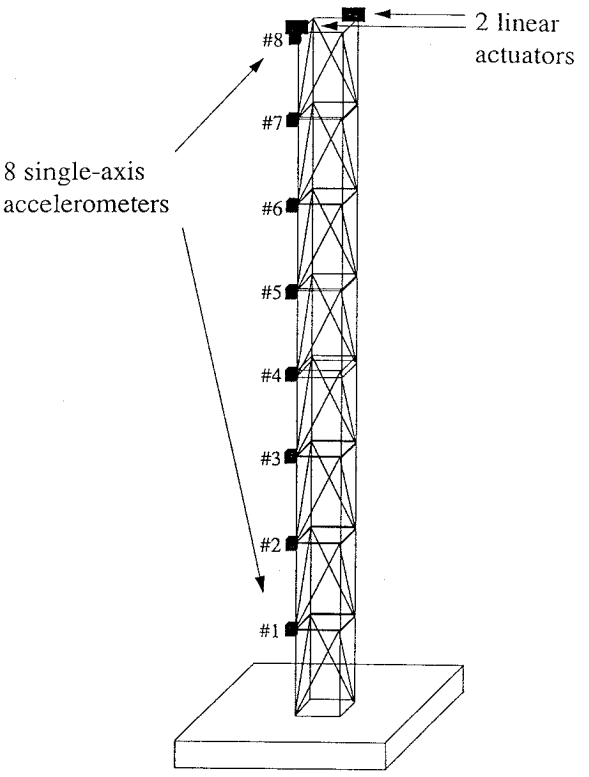

Fig. 1 6-m FTE.

Truss Description

The basic structure of the experiment is a lightly damped 6-m truss, cantilevered vertically from a rigid support base. The FTE is depicted in Fig. 1. The truss is composed of two equal length frames of welded tubular aluminum alloy longerons and battens with bolt-in tubular Lexan diagonals in a back-to-back K pattern. The assembled truss has a square cross section of 20 in. on a side. The longerons are made from 6061-T6 aluminum alloy tubes with a 1.5-in.-square cross section and 0.065-in. wall thickness. The battens are 6061-T6 tubes with 0.5-in.-square cross section and 0.063-in. wall thickness. The diagonal members are Lexan tubing (270,000 psi elastic modulus) with a 1.5-in.-diam circular cross section with 0.125-in. wall thickness. The diagonals have aluminum end fittings that are fastened to the truss with two bolts and a half-clevis joint at both ends. The truss has four bays in each of the two sections for a total of eight bays. The two sections are bolted together with two bolts at each longeron end. Four bolts at the base of each longeron secure the truss to a 1-in.-thick aluminum plate that is securely bolted to the laboratory floor.

Actuators—Sensors and Supporting Equipment

Input excitation to the truss for frequency response testing is provided through the use of two linear momentum exchange (reaction mass) actuators. Each actuator is capable of approximately 1-lbf peak output. Power is provided to the actuators by individual current drive circuits. The actuators use a linear dc motor with the armature fixed to a base and the permanent magnetic field suspended on shafts and linear bearings. Two linear springs provide the centering force for the mass. The resonant frequency for each actuator is approximately 0.9 Hz, with an effective viscous damping ratio of approximately 10% of critical. For comparison, the fundamental

frequency of the truss is approximately 7 Hz. Mounting plates were fabricated to attach the actuators atop two longerons on the free end of the truss. Driving the actuators in phase with one another excites the bending modes in one axis. The torsional modes are excited by driving the actuators 180 deg out of phase.

Acceleration measurements are made using eight Sunstrand QA-1400 single-axis inertial accelerometers. These accelerometers were chosen for their high sensitivity and low noise characteristics. The eight accelerometers were placed along one longeron at the node location at each bay. For signal processing, a Tektronix 2642A Fourier Analyzer is used to measure and average the frequency response functions.

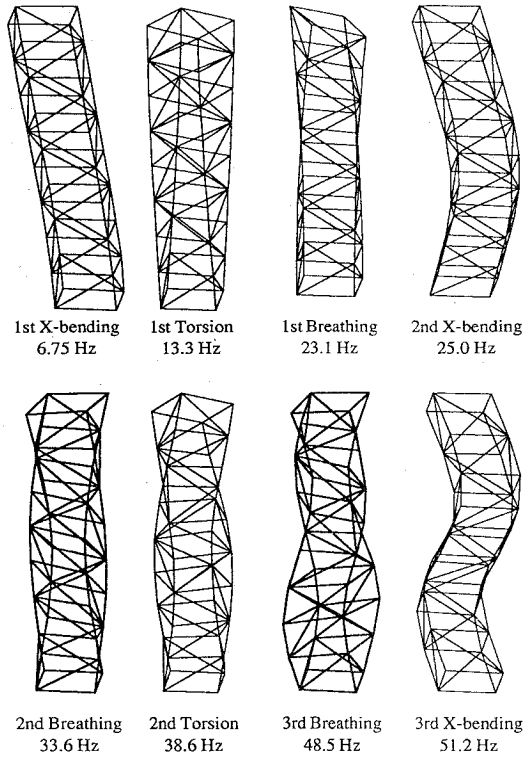

Fig. 2 Low-frequency mode shapes for the FTE.

Finite Element Model

The FTE was modeled in ASTROS using four different types of beam elements for a total of 100 elements. The four types were aluminum vertical longeron elements, aluminum horizontal batten elements, Lexan diagonal elements, and aluminum horizontal midsection elements. Lumped masses were included to account for the actuators, top plates (actuator attach points), K brackets (used to secure the diagonal members), and midplates (bolt assemblies used to secure the two four-bay sections together). Care was taken to accurately obtain the mass properties, area properties, and moments of the structural elements. The elastic properties were determined from laboratory tests on individual elements. These parameters were all used to construct a baseline data deck for input into ASTROS. Using the results of the baseline finite element analysis along with software written in MATLAB[20] to display and animate mode shapes, a characterization of the low frequency (below 70 Hz) behavior of the FTE was performed. Mode shapes were classified as X bending, Y bending, torsion, and breathing. Eight low-frequency mode shapes are shown in Fig. 2. Because of the near symmetry, the Y-bending mode shapes are similar to the X-bending shapes and are not shown. The next step was to compare the analytical results to measured data.

Testing Procedure

Experimental measurements were performed on the FTE using random vibration testing. The vibration test was performed by exciting the actuators with a band-limited (0–100 Hz) random noise sequence. Frequency averaged transfer functions between the input excitation and the eight accelerometers were measured. The inverse discrete Fourier transformations of these transfer functions yielded the impulse response functions that were input into an eigensystem realization algorithm (ERA)[21,22] to obtain measured modal frequencies and shapes. Because of the fixed location of the sensor and actuators, only X-bending and torsion modes could be directly excited and measured. The experimental data set consisted of the frequencies and partial mode shapes for the first three X-bending modes, as well as the frequencies for the first three torsional modes. The X-bending partial mode shapes consisted of eight measurements, normalized such that the maximum entry for each mode was unity. The eight measurements per mode corresponded to the nodal DOFs along the single instrumented longeron. Distinguishing between bending modes and breathing modes was easily facilitated by exciting the structure in both bending (actuators in phase) and torsion (actuators 180 deg out of phase). Figure 3 shows the resulting output at accelerometer no. 8 for the two different types of excitation.

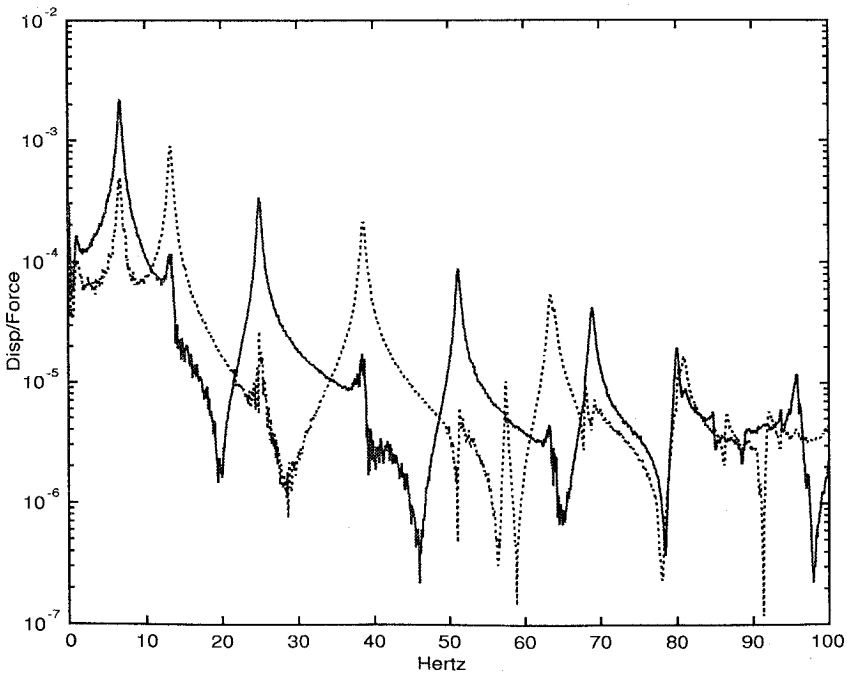

Fig. 3 Comparison of bending and torsional excitation on the FTE: ——, bending input; and - - - -, torsional input.

Table 1 Analytical and measured natural frequencies of FTE

Mode no.	Description	Frequency, Hz			
		Experimental	Analytical	Initial tuning	Final tuning
1	First Y bending	——	6.43	6.60	6.48
2	First X bending	6.75	6.52	6.75	6.64
3	First torsion	13.34	10.93	13.32	13.09
4	First breathing	23.1	17.72	19.68	22.65
5	Second Y bending	——	23.32	24.58	24.80
6	Second X bending	24.98	23.48	24.97	25.29
7	Second breathing	33.6	30.33	31.09	32.91
8	Second torsion	38.66	32.09	38.71	38.46
9	Third Y bending	——	48.66	50.29	50.95
10	Third X bending	51.21	49.06	51.20	51.93
11	Third breathing	48.5	52.35	54.97	53.92
12	Third torsion	63.53	56.17	63.80	63.02

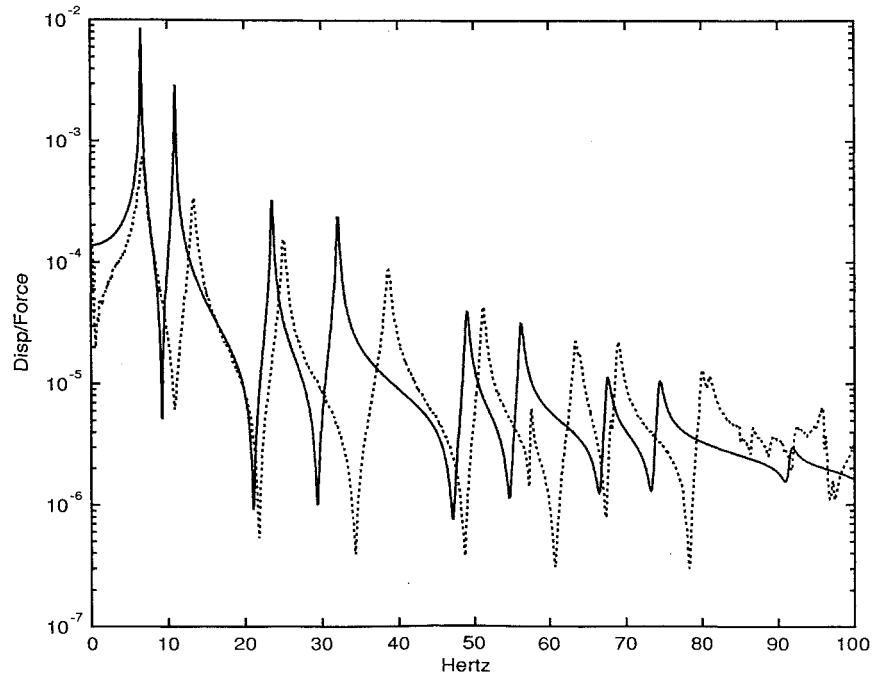

Fig. 4 Comparison of initial analytical model and measured frequency response: - - - -, measured; and ——, FE baseline.

Model Tuning Results

Despite the effort expended in constructing the baseline finite element model of the FTE, it did not agree well with the measured data. The poor correlation between the baseline analytical and measured data is depicted in Fig. 4, which shows the transfer function between a colocated sensor (accelerometer 8) and actuator at the top of the FTE. Before computing the transfer functions, damping was included in the analytical model by assuming a value of one-half of 1% of critical damping for all modes (a typical measured value). This was done only to avoid the unbounded resonant spikes due to an undamped model, and thus the height of the resonant peaks between analytical and measured data is insignificant. It is clear from Fig. 4 that the baseline FEM does not adequately represent the measured dynamic characteristics of the FTE and would hence benefit greatly from model tuning.

Using the tuning procedure described earlier, the baseline FEM was tuned to the measured data. For the initial tuning, the frequencies and partial mode shapes of the three X-bending modes and the frequencies of the three torsional modes were included in the objective function. The design variables chosen were the mass and elastic modulus of the four different types of beam elements and the mass value of the lumped masses used for the actuators, top plates, K brackets, and midplates. Symmetry was maintained by linking all like elements to the same design parameter. All total, 12 design variables were used. The tuning process converged in six outer-loop iterations. Convergence was defined as a less than one-half of 1% change in the objective function value between two consecutive outer-loop iterations. The results of this initial tuning are shown in Fig. 5 for the same actuator/sensor combination as used in Fig. 4. The results show excellent agreement over the 60-Hz frequency band covered in the objective function. Table 1 lists the frequencies for the first 12 modes based on measured data, the analytical baseline, and the tuned FEMs. Table 2 lists the resulting changes in the design variables in the tuned model. The values in Table 2 indicate the fraction of the tuned values relative to the baseline values.

The objective function, Eq. (1), included terms a_i and b_{ij} to weight individual contributions to the overall value. For the initial tuning all a_i coefficients were set to 100 and all b_{ij} were set to unity. This represents equal confidence in the measurement data for all frequencies included, with a stronger emphasis placed on tuning the modal frequencies rather than tuning the shapes. In general, selection of the weighting coefficients is dependent upon the confidence with which each mode is measured, as well as the designer's desire to minimize a selected portion of the correlation error. For this test case, emphasis was placed on minimizing the frequency correlation errors.

A key aspect in the tuning process is the ability to detect and account for mode switching. To tune the FTE model, the first 20 modes were selected for the eigenanalysis. It is important to include an adequate number of modes when computing Eq. (13) because mode switching can only be detected between modes included in the correlation coefficient matrix. Mode switching was detected between mode numbers 13–20 during the tuning process; however, these

modes were not used in the objective function. Mode switching did not occur between the first 12 modes. To further test the mode switch tracking capability, a test was performed by tuning the model to the measured frequencies for modes 10 and 11 only. Note that the 10th (3rd X bending) mode measured was higher in frequency than the 11th (3rd breathing) mode. When tuning on only these two frequencies, a mode swap was detected after the first iteration, and the model was successfully tuned to both frequencies. The ordering of these two modes also illustrates the importance of performing a preliminary correlation analysis to match measured and initial FEM modes.

Off-Nominal Simulations

As initially discussed, the impetus in tuning analytical models to measured data is to have the capability to simulate and predict the dynamic behavior of large flexible structures. Particularly important

Table 2 Design variable values in the FTE FEM

Design variable no.	Description	Variation from initial value: Initial tuning	Variation from initial value: Final tuning
1	Longerons (elastic modulus)	0.83	0.80
2	Battens (elastic modulus)	0.90	1.47
3	Midbattens (elastic modulus)	0.93	1.7
4	Diagonals (elastic modulus)	1.40	1.59
5	Longerons (mass)	0.29	0.80
6	Battens (mass)	1.35	1.22
7	Midbattens (mass)	1.12	0.83
8	Diagonals (mass)	3.18	1.69
9	K brackets (mass)	1.01	1.77
10	Actuators (mass)	0.5	0.5
11	Midplates (mass)	0.87	0.5
12	Topplates (mass)	0.64	0.75

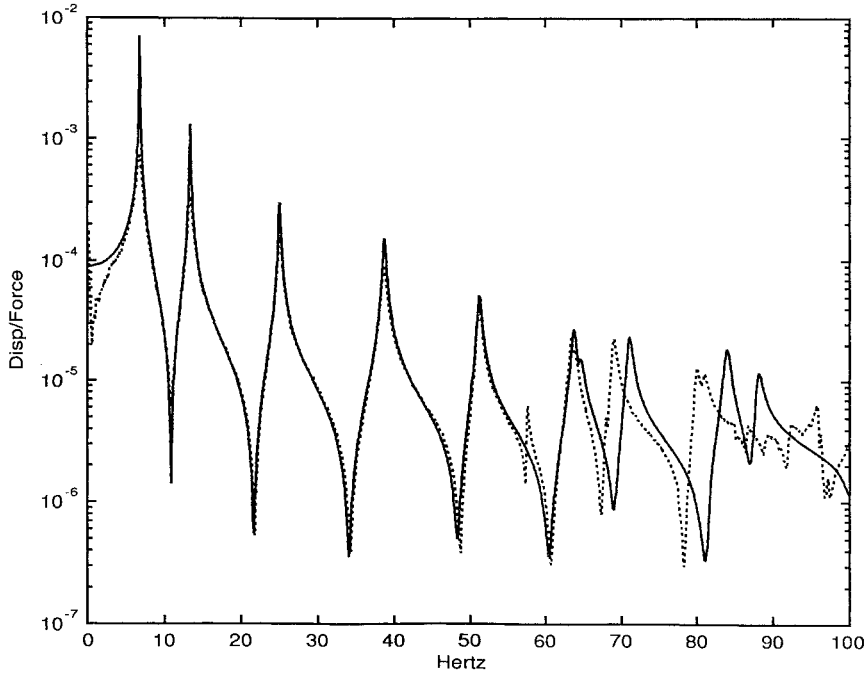

Fig. 5 Comparison of the tuned analytical model and measured frequency response, initial tuning: - - - -, measured; and ——, FE tuned.

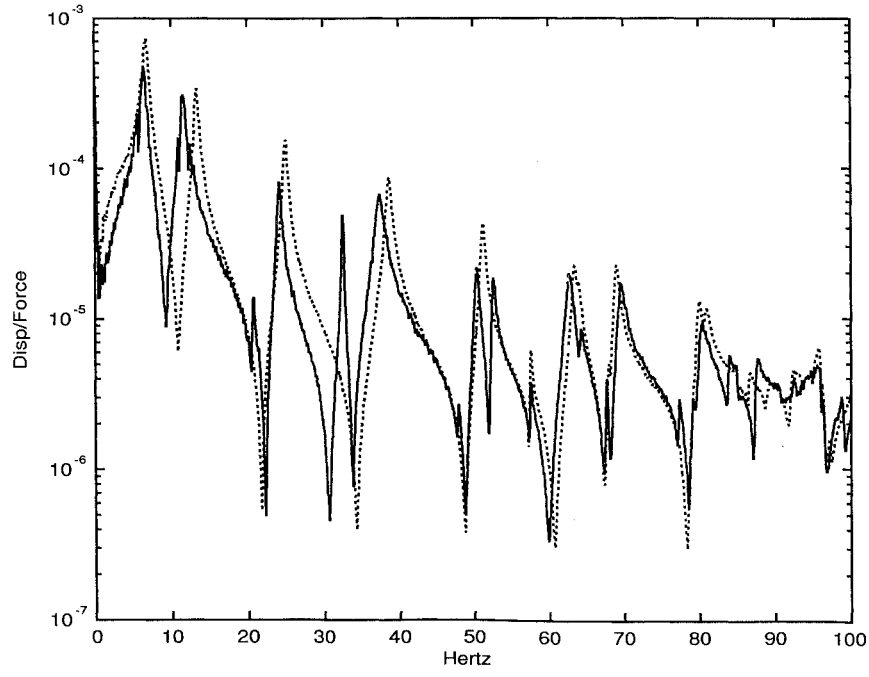

Fig. 6 Effect of structural damage on the measured response: - - - -, nominal; and ——, damaged.

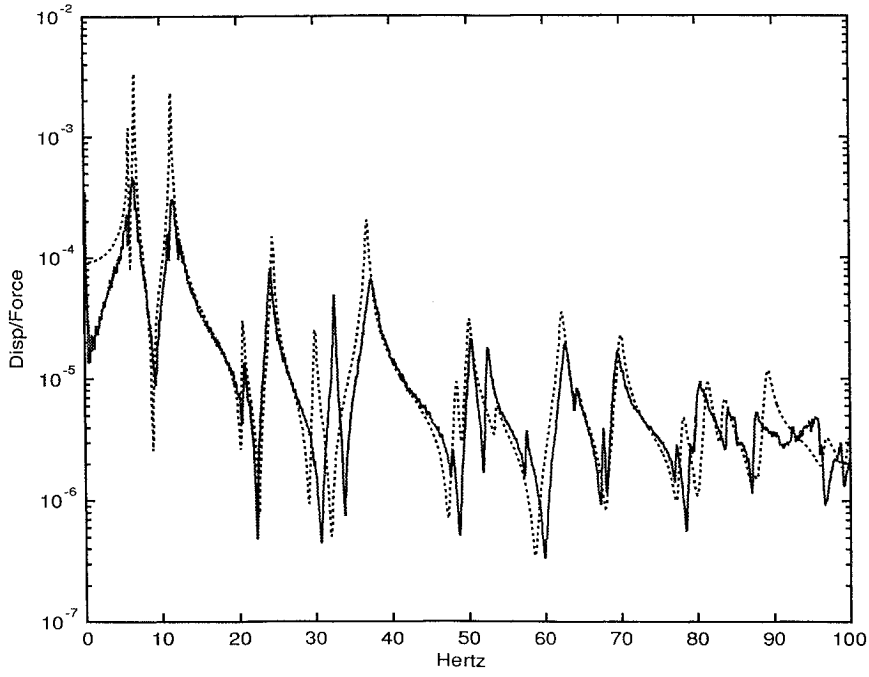

Fig. 7 Comparison of simulated damage and measured data on the damaged FTE: ——, measured; and - - - -, FE simulated.

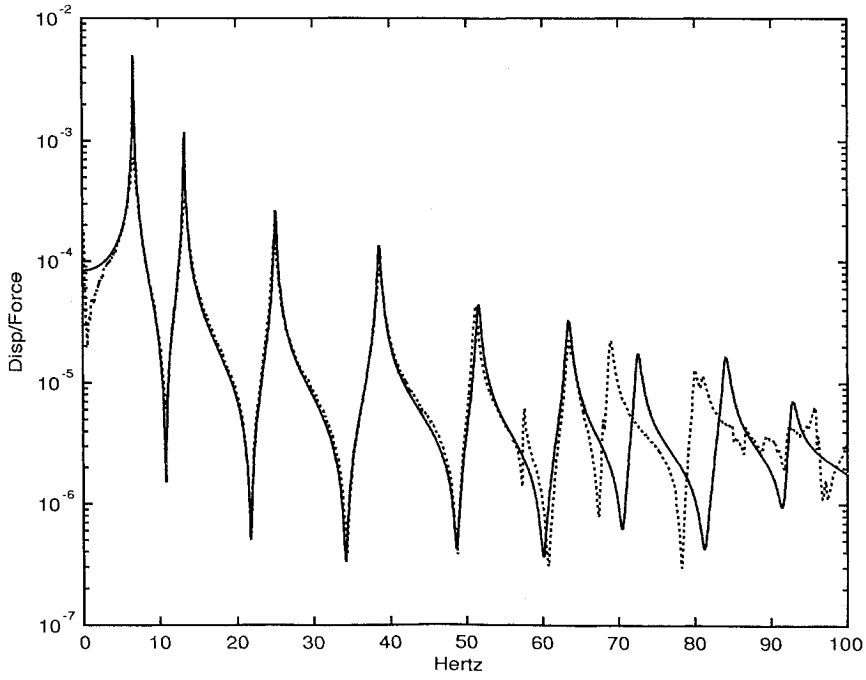

Fig. 8 Comparison of the tuned analytical model and measured frequency response, final tuning: - - - -, measured; and ——, FE tuned.

is the simulations of off-nominal conditions, which can arise due to several factors including damage, aging, manufacturing variability, etc. To verify the off-nominal simulation capability, a single diagonal Lexan strut was removed from the FTE to simulate a damaged configuration. The subsequent change in the measured frequency response is illustrated in Fig. 6. The figure shows a significant shift in the torsional modes, as well as the appearance of the breathing modes ($\approx$23 and $\approx$33 Hz). In the undamaged structure, these breathing modes were not detectable from this particular sensor/actuator pair.

For the tuned FEM to prove its worth as a simulation tool, removing the same diagonal Lexan beam element from the model should produce the same frequency response as was measured on the damaged FTE (in the frequency range for which the model was tuned). The results of this comparison are shown in Fig. 7. A significant disagreement is evident in the second breathing mode ($\approx$33 Hz). To correct this disagreement, the initial FEM was retuned using the frequencies of the first three breathing modes in addition to the measured bending and torsional data used previously. Because the breathing modes are difficult to excite and measure with the chosen sensor actuator locations, the weighting on these frequencies in the objective function was set one order of magnitude lower (10 vs 100) than used for the other frequency measurements. This reflects the lower confidence placed on these measurements.

The results of retuning the model using the additional measurements appear almost identical to the results of the initial tuning and are shown in Fig. 8. Now, however, when the structural damage is simulated, the FEM accurately matches the measured results of the damaged FTE. This is shown in Fig. 9. This illustrates the importance of including sufficient data in the tuning process to

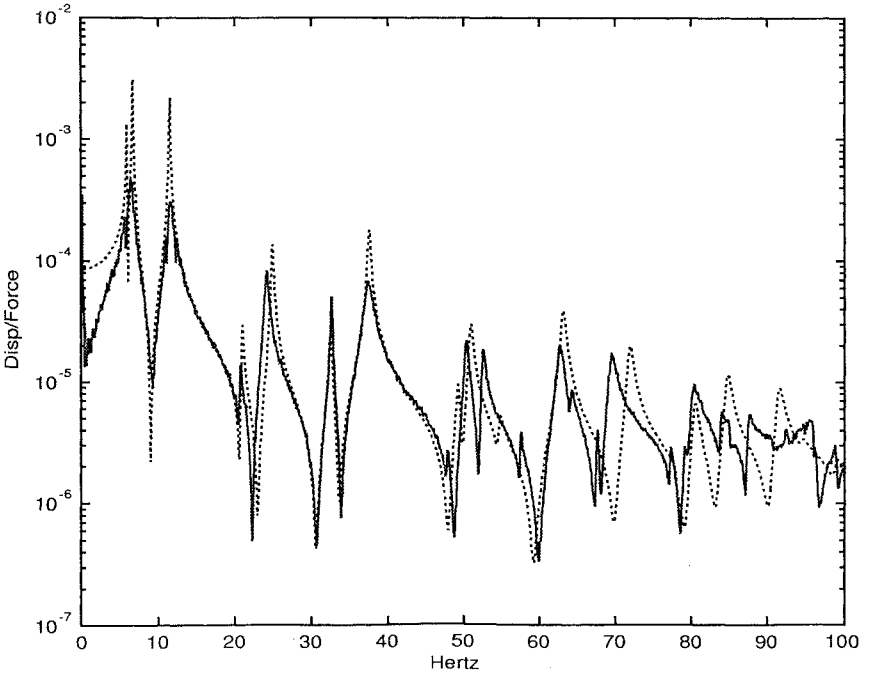

Fig. 9 Comparison of simulated damage and measured data on the damaged FTE with additional tuning constraints: ——, measured; and - - - -, tuned FE.

achieve the desired simulation results. It also demonstrates the importance of verifying off-nominal behavior in the model validation process. Again, the frequencies and resulting design variable values are shown in Tables 1 and 2, listed under final tuning. Note that the initial and final tuning are two independent test cases. The data for the final tuning included the first three breathing modes in addition to the torsion and bending data used in the initial tuning. Comparing the initial and final tuning frequency values against the measured values in Table 1, it is clear there is a tradeoff. The breathing modes now more closely match the measured values with some degradation in the match of the bending and torsion modes. As with any objective function optimization, increasing the number of constraints, without increasing the number of design variables, will in general not be able to simultaneously satisfy all constraints.

Conclusions

An algorithm was developed to tune FEMs to measured eigendata. Careful attention was placed on eigenvector normalization and how the normalization relates to the computation of the eigenvalue and eigenvector sensitivities. Mode switches were successfully tracked through an analysis of the correlation coefficient matrix. This algorithm was implemented using ASTROS and was demonstrated by tuning a 100-element FEM of an experimental flexible frame structure. The results clearly demonstrate the capability of this method. In addition, the importance of validating off-nominal simulations was presented. Implementation of this algorithm in ASTROS makes this tuning procedure readily accessible to the design engineer during the finite element design phase. This level of experimentally validated automated tuning represents a substantial improvement over current capabilities. Natural applications of this algorithm include the identification of uncertain structural parameters, as well as the identification of damaged structural elements.

References

[1]Stiles, P. A., and Kosmatka, J. B., "Comparison of Model Refinement Techniques," AIAA Paper 89-1279, April 1989.

[2]Chen, J. C., and Garba, J. A., "Analytical Model Improvement Using Modal Test Results," *AIAA Journal*, Vol. 18, No. 6, 1980, pp. 684–690.

[3]Grossman, D. T., "An Automated Technique for Improving Modal Test/Analysis Correlation," AIAA Paper 82-0604, May 1982.

[4]Hemez, F., and Farhat, C., "Locating and Identifying Structural Damage Using a Sensitivity-Based Model Updating Methodology," *Proceedings of the AIAA/ASME/ASCE/AHS/ASC 34th Structures, Structural Dynamics, and Materials Conference*, AIAA, Washington, DC, 1993, pp. 2641–2653.

[5]Doebling, S. W., "Selection of Experimental Modal Data Sets for Damage Detection via Model Update," *Proceedings of the AIAA/ASME/ASCE/AHS/ASC 34th Structures, Structural Dynamics, and Materials Conference*, AIAA, Washington, DC, 1993, pp. 1506–1517.

[6]Berman, A., and Nagy, E. J., "Improvement of a Large Analytical Model Using Test Data," *AIAA Journal*, Vol. 21, No. 8, 1983, pp. 1168–1173.

[7]Baruch, M., "Optimal Correction of Mass and Stiffness Matrices Using Measured Modes," *AIAA Journal*, Vol. 20, No. 11, 1982, pp. 1623–1626.

[8]Kabe, A., "Stiffness Matrix Adjustment Using Mode Data," *AIAA Journal*, Vol. 23, No. 9, 1985, pp. 1431–1436.

[9]Kammer, D. C., "Optimum Approximation for Residual Stiffness in Linear System Identification," *AIAA Journal*, Vol. 26, No. 1, 1988, pp. 104–112.

[10]Smith, S. W., and Beattie, C. A., "Secant-Method Adjustment for Structural Models," *AIAA Journal*, Vol. 29, No. 1, 1991, pp. 119–126.

[11]Chen, J. C., and Garba, J. A., "On-Orbit Damage Assessment for Large Space Structures," *AIAA Journal*, Vol. 26, No. 9, 1988, pp. 1119–1126.

[12]Niell, D. J., and Herendeen, D. L., "ASTROS User's Manual," Wright Lab., WL-TR-93-3025, Wright–Patterson AFB, OH, March 1993.

[13]Gibson, W. C., "ASTROS-ID: Software for System Identification Using Mathematical Programming," Wright Lab., WL-TR-91-3101, Wright–Patterson AFB, OH, Sept. 1992.

[14]Plaut, R. H., and Huseyin, K., "Derivatives of Eigenvalues and Eigenvectors in Non-Self-Adjoint Systems," *AIAA Journal*, Vol. 11, No. 2, 1973, pp. 250, 251.

[15]Fox, R. L., and Kapoor, M. P., "Rates of Change of Eigenvalues and Eigenvectors," *AIAA Journal*, Vol. 6, No. 12, 1968, pp. 2426–2429.

[16]Nelson, R. B., "Simplified Calculation of Eigenvector Derivatives," *AIAA Journal*, Vol. 14, No. 9, 1976, pp. 1201–1205.

[17]Neill, D. J., Johnson, E. J., and Canfield, R. A., "ASTROS—A Multidisciplinary Automated Structural Design Tool," *Journal of Aircraft*, Vol. 27, No. 12, 1990, pp. 1021–1027.

[18]Lou, X., and Grandhi, R. V., "ASTROS for Reliability-Based Multidisciplinary Structural Analysis and Optimization," *Proceedings of the AIAA 36th Structures, Structural Dynamics, and Materials Conference*, AIAA, Washington, DC, 1995, pp. 93–102.

[19]Gordon, R. W., "The Twelve-Meter Truss Active Control Experiment Design, Analysis and Open Loop Testing," Wright Lab., WL-TR-92-3012, Wright–Patterson AFB, OH, April 1992.

[20]Anon., "MATLAB: High Performance Numeric Computation and Visualization Software," The Math Works, Inc., Natick, MA, 1994.

[21]Cobb, R. G., and Liebst, B. S., "Structural Damage Identification from Frequency Response Data," *Proceedings of the 1995 Guidance, Navigation, and Control Conference* (Baltimore, MD), AIAA, Washington, DC, 1995, pp. 334–344.

[22]Juang, J., and Pappa, R. S., "An Eigensystem Realization Algorithm for Modal Parameter Identification and Model Reduction," *Journal of Guidance, Control, and Dynamics*, Vol. 8, No. 5, 1985, pp. 620–627.